

The inner ~ 40 pc Radial Distribution of the Star formation Rate for a nearby Seyfert 2 galaxy M51

Li-Ling Fang, Xiao-Lei Jiang, Zhi-Cheng He and Wei-Hao Bian¹

Department of Physics and Institute of Theoretical Physics, Nanjing Normal University, Nanjing 210046, China; whbian@njnu.edu.cn

Received [year] [month] [day]; accepted [year] [month] [day]

Abstract We investigate spatially resolved specific star formation rate (SSFR) in the inner ~ 40 pc for a nearby Seyfert 2 galaxy, M51 (NGC 5194) by analyzing spectra obtained with the *Hubble Space Telescope* (HST) Space Telescope Imaging Spectrograph (STIS). We present 24 radial spectra measured along the STIS long slit in M51, extending $\sim 1''$ from the nucleus (i.e., -41.5 pc to 39.4 pc). By the simple stellar population synthesis, the stellar contributions in these radial optical spectra are modeled. Excluding some regions with zero young flux fraction near the center (from -6 pc to 2 pc), we find that the mean flux fraction of young stellar populations (younger than 24.5 Myr) is about 9% , the mean mass fraction is about 0.09% . The young stellar populations are not required in the center inner ~ 8 pc in M51, suggesting a possible SSFR suppression in the circumnuclear region (~ 10 pc) from the feedback of active galactic nuclei (AGNs). The radial distribution of SSFR in M51 is not symmetrical with respect to the long slit in STIS. This unsymmetrical SSFR distribution is possibly due to the unsymmetrical AGN feedback in M51, which is related to its jet.

Key words: galaxies:active—galaxies:Seyfert—galaxies:starburst

1 INTRODUCTION

The star formation history in galaxies is intimately related to the galaxy evolution, as well to the evolution of central super massive black holes (e.g. Kennicutt, 1998; Tremaine, 2002; Asari et al., 2007; Chen et al., 2009). It has been suggested that star formation in circumnuclear regions in Seyfert galaxies is suppressed (e.g. Wang et al., 2007). Also, specialists in this field have found that there is a correlation between the mean specific star formation rate and the Eddington ratio, suggesting that active galactic nuclei (AGNs) are possibly triggered by supernova explosions in the circumnuclear regions (e.g. Chen et al., 2009).

With high angular resolution, radial spectra obtained with *Hubble Space Telescope* (HST) Space Telescope Imaging Spectrograph (STIS) provide unique information on the host and central accretion processes in active galaxies (e.g. Spinelli et al. 2006; Rice et al. 2006). For some nearby Seyfert 2 galaxies, their central engines are obscured by a torus, which enhances the contrast between the stellar light from their host and the nuclear continuum from the central accretion disk. In order to investigate radial star formation rate in circumnuclear regions of AGNs, a nearby Seyfert 2 galaxy, M51, is selected, and spectra from its central region (~ 40 pc) obtained from *HST* STIS are analyzed.

The paper is organized as follows: Section2 presents the data reduction and the radial spectra. Section3 models the spectra by simple stellar population synthesis (SSPS). Section4 includes our discussion and results.

Table 1 M51 observations by HST STIS.

Data	dataset	Exposure Time	Grating	Aperture	Center Wavelength	$\Delta\lambda$
1998 Apr 2	O4R401090	1858 s	G430M	52" \times 0."2	4961Å	282Å
1998 Apr 2	O4R4010A0	600 s	G430M	52" \times 0."2	4961Å	282Å
1998 Apr 2	O4R4010B0	2066 s	G430L	52" \times 0."2	4300Å	2807Å
1998 Apr 2	O4R4010C0	1020 s	G430L	52" \times 0."2	4300Å	2807Å
1998 Apr 2	O4R4010D0	1644 s	G750L	52" \times 0."2	7751Å	4987Å
1998 Apr 2	O4R4010E0	25 s	G750L	52" \times 0."2	7751Å	4987Å

2 DATA REDUCTION

2.1 HST STIS data

M51 (NGC 5194) is a nearby Seyfert 2 galaxy with $z=0.0015$ (e.g., Spinelli et al. 2006). Searching the *HST* archive for M51, there are six datasets observed by STIS, i.e., two by G430M, two by G430L, two by G750L (Table 1). Checking these data, we find that two datasets (i.e., O4R4010B0 by G430L and O4R4010D0 by G750L) acquired in low dispersion grating modes are suitable for host stellar population analysis, which provides continuous wavelength coverage spanning the spectral region from 2900 Å to $1\mu m$ (e.g. Bradley et al., 2004). The dataset by G430M has very narrow wavelength coverage ($\sim 4800\text{Å}-5100\text{Å}$), which is not suitable for SSPs. The STIS plate scale is $0.05078''\text{pixel}^{-1}$ and the slit length is $50''$. Given the distance to M51 of 8.4 Mpc, $1''$ corresponds to 40.7 pc and 1 pixel corresponds to 2.07 pc.

These STIS datasets by G430L and G750L give high spatial resolution ($0.1''$, or 4.1 pc) spectra in the central region of M51. The spectra were acquired through a $52'' \times 0.''2$ orientation at a single position angle of 166° , and the radio structure is elongated along a position angle of 166° (east of north, Bradley et al. 2004). The $0.2''$ wide slit was projected onto 3.75 STIS CCD pixels, which corresponds to spectral resolutions of 10.3 Å for G430L and 18.3 Å for G750L (e.g. Bradley et al., 2004).

Because the active nucleus of M51 is obscured, which is expected for a Seyfert 2 galaxy, the AGN continuum is not apparent in our lower resolution G430L and G750L spectra. Instead, the circumnuclear spectra exhibit strong stellar population in the M51 host galaxy.

2.2 Data reduction in IRAF

From STIS website, calibrated files were downloaded, as well as the reference files. Following STIS Data Handbook, one-dimensional spectra were extracted from the two-dimensional spectra using the CALSTIS `x1d` routine, which performs a geometric rectification and background subtraction. In order to investigate the radial spectra at different distances from the nucleus, we extracted spectra at different positions and with different sizes of the extraction box, in reference pixels. Following Bradley et al. (2004), the nucleus of M51 was selected between cloud 4 and cloud 5 (these clouds correspond to the narrow line regions in M51).

For STIS grating modes G430L and G750L, we extracted spectra at the same positions with the same sizes as the extraction boxes. For G430L spectra, the wavelength coverage was 2901 Å– 5709 Å, and for G750L spectra, it was 5267 Å– 10258 Å. Considering the balance between the number of radial spectra and the spectral signal-to-noise ratio (snr), the extraction box was from 1 to 4 pixels, corresponding to angular sizes of $0.051'' - 0.204''$ (line 3 in Table 2). There were 24 spectra extracted at both sides of the nucleus, extending $\sim 1''$ (40.7 pc) from the nucleus (Fig. 1, 2).

2.3 Simple Stellar Population Model

Spectra acquired by G430L and G750L have different wavelength coverages. However, there is an overlap between the spectra acquired by G430L and G750L. We used the following step to process data from

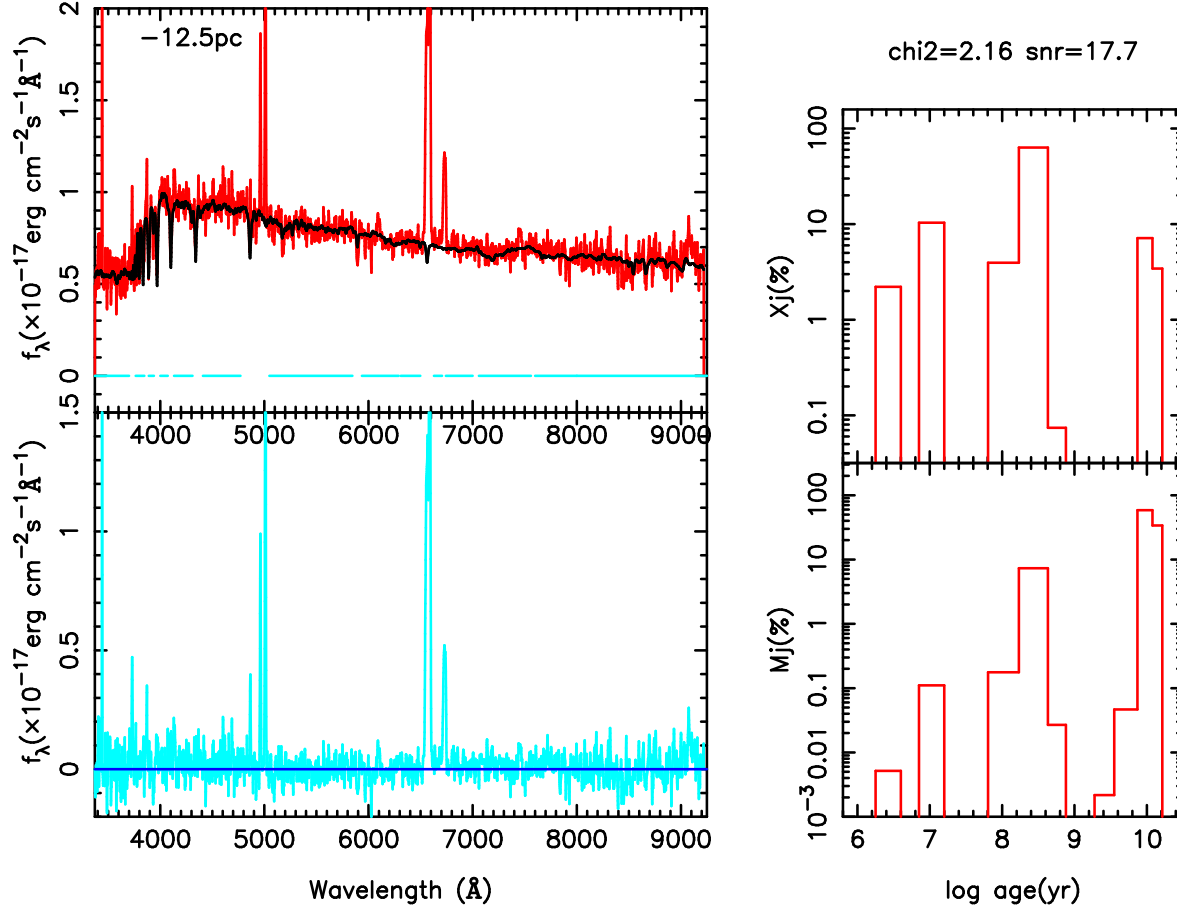


Fig. 1 An example of the simple stellar population synthesis for a spectrum separated from the nucleus by -12.5 pc. Top left: Observed (the red line) and model (the black line) spectra. Cyan line in the bottom indicates the fit windows. Bottom-left: Residual spectrum. Right: the distributions of flux fraction (top) and mass fraction (bottom) as a function of stellar age. The reduced χ^2 and snr are given at the top of the right panel.

Simple Stellar Population (SSP) model. First, all spectra were resampled with $\Delta\lambda = 1 \text{ \AA}$. Second, the spectra acquired by G750L were scaled to have the same mean flux as those by G430L in their common wavelength range of $5500 \text{ \AA} - 5600 \text{ \AA}$. For this common wavelength range, we used the spectra by G430L. Then we obtained 24 radial spectra from M51, with a wavelength coverage of $2901 \text{ \AA} - 10258 \text{ \AA}$ (Fig. 1 and 2).

We use SSP synthesis (STARLIGHT; Cid Fernandes et al., 2005) to model the stellar contribution in the Galactic extinction-corrected spectrum in the rest frame (Cid Fernandes et al., 2005; Bian & Huang, 2010). The Galactic extinction law of Cardelli et al. (1989) with $R_V = 3.1$ is adopted. There are three files used by the code STARLIGHT, i.e., a base-file, a configuration file and a mask-file for emission lines. The configuration file contains all of the technical parameters which control STARLIGHT, including the clipping threshold, limits for extinction and kinematical parameters, and limits for the intrinsic extinction.

We use 45 default templates in Cid Fernandes et al. (2005), which are calculated from the model of Bruzual & Charlot (2003) with a spectral interval of 1\AA between 3322\AA to 9300\AA . The linear combination of 45 templates is used to represent the host bulge spectrum. These 45 templates are comprised of 15 ages, from 1 Myr to 13 Gyr, i.e., $t = 0.001, 0.00316, 0.00501, 0.01, 0.02512, 0.04, 0.10152, 0.28612, 0.64054, 0.90479, 1.434, 2.5, 5, 11$ and 13 Gyr, and three metallicities, $Z = 0.2, 1$ and $2.5 Z_{\odot}$ (Cid Fernandes et al. 2005). At the same time as the SSP fit, we add a power-law component with a fixed slope of -0.5 ($f_{\lambda} \propto \lambda^{-0.5}$) in the code to represent the AGN continuum emission. Information about these 45 templates is listed in the base-file, which is used in STARLIGHT.

The synthetic spectrum is built using the following equation,

$$M_{\lambda} = M_{\lambda_0} \left(\sum_{j=1}^{N_*} x_j b_{j,\lambda} r_{\lambda} \right) \otimes G(v_0, v_d) \quad (1)$$

where $b_{j,\lambda}$ is the j^{th} template normalized at $\lambda_0 = 4020\text{\AA}$, x_j is the flux fraction at 4020\AA , M_{λ_0} is the synthetic flux 4020\AA , $r_{\lambda} \equiv 10^{-0.4(A_{\lambda} - A_{\lambda_0})}$ is the reddening term by V-band extinction A_V adopted for the Galactic extinction law, and $G(v_0, v_d)$ is the line-of-sight stellar velocity distribution, modeled as a Gaussian centered at velocity v_0 and broadened by the velocity dispersion v_d . The limit is from 0 to 500 km s^{-1} for v_d , from -500 to 500 km s^{-1} for v_0 , from 0 to 5 mag for A_V , which are listed in the configuration file.

We exclude the AGN emission lines in the mask-file, such as H Balmer lines, [O II] $\lambda 3727$, [Ne III] $\lambda 3869$, [O III] $\lambda \lambda 4959, 5007$, [N II] $\lambda \lambda 6548, 6583$, and [S II] $\lambda \lambda 6717, 6731$. We also limit rest-frame wavelength range from 3372\AA to 9000\AA to match the SSP templates.

The best fit is reached by minimizing reduced χ^2 between the observed spectrum and the model spectrum with a simulated annealing plus Metropolis scheme. An example fit is shown in Fig. 1.

3 RESULTS AND DISCUSSION

3.1 The flux/mass fraction for young stellar populations

Through above spectral synthesis, we can obtain flux-fraction x_j and mass-fraction μ_j for different stellar populations of ages and metallicities. The mass-flux ratio can be found in the STARLIGHT manual on the webpage, <http://astro.ufsc.br/starlight/>. A SSP model for a spectrum taken from a point away from the nucleus by -12.5 pc is shown in Fig. 1. The red curve is the observed *HST* STIS spectrum by G430L and G750L. On top left panel in Fig.1, the black curve is the SSP fit with linear combination of different stellar population templates. In the bottom left panel, the cyan curve is the residuals. The right panel shows the distribution of flux fraction as function of the age of stellar population plates (top), and the corresponding distribution of mass fraction (bottom). SSP models for all of the 24 radial spectra are presented in Fig.2. Fig. 3 is the same as Fig. 2 but for the spectral region of $3700\text{-}4200\text{\AA}$ in detail.

Properties of 24 radial spectra of M51 are presented in Table 2. These properties are described as follows. Line 1 (top line): the sequence number of radial spectrum; line 2: the distance from the nucleus in the unit of pc; line 3: the size of extraction box in pixels; line 4: the snr of radial spectrum; line 5: reduced χ^2 of SSP fit; line 6: the intrinsic extinction; line 7: the flux fraction of power law component; line 8: the flux fraction of young stellar population ($t < 0.102\text{ Gyr}$); line 9: the flux fraction of young stellar population ($t < 24.5\text{ Myr}$); line 10: the mass fraction of young stellar population ($t < 0.102\text{ Gyr}$); line 11: the mass fraction of young stellar population ($t < 24.5\text{ Myr}$).

In Table 2, the intrinsic extinction is needed in the fit, from 0.37-1.46. Regarding the age-metallicity degeneracy, Cid Fernandes et al. (2005) mentioned that this problem is presented in STARLIGHT and introduces systematic biases in age and Z estimates of up to 0.1-0.2 dex. From results of the simulation by Cid Fernandes et al. (2005), it is suggested that the uncertainty in SSP results can be given by the effective starlight snr at 4020\AA in three age bins, i.e., "young" ($t < 0.1\text{ Gyr}$), "intermediate" ($0.1\text{ Gyr} \leq t \leq 1\text{ Gyr}$), and "old" ($t > 1\text{ Gyr}$). For the "young" age bin, the errors in flux/mass fraction are much smaller than those in the ages of "intermediate" and "old". For our spectra, the effective starlight snr at

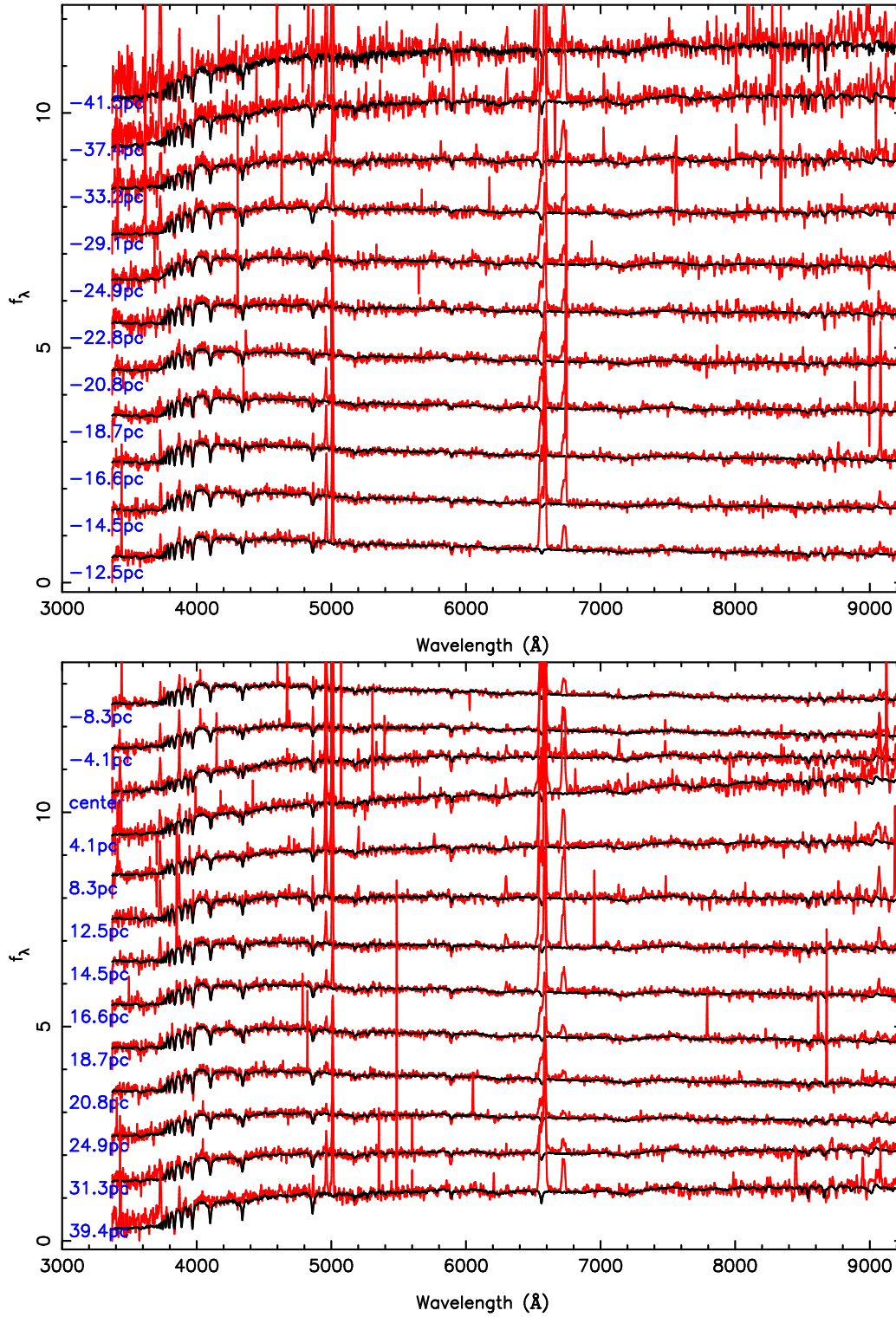


Fig. 2 All of 24 radial spectra with their SSP models, from -41.5 pc to 39.4 pc. The red lines are the observed spectra and the black lines are the model spectra. The distance from the nucleus is presented at the left of each spectrum.

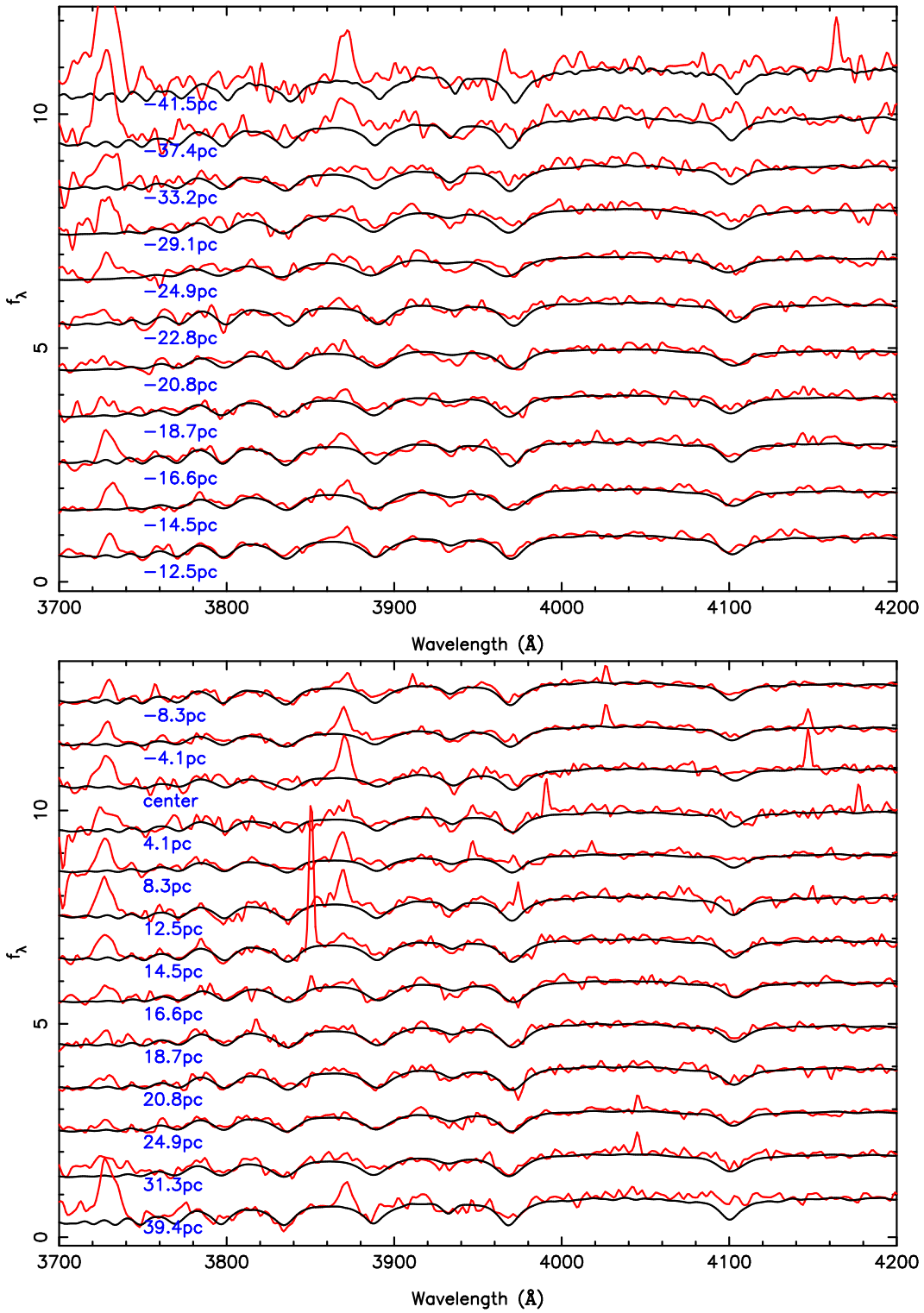


Fig. 3 Same as Fig. 2 but for the spectral region of 3700-4200 \AA .

Table 2 The properties of 24 radial spectra in M51. For the last four lines, young_x1 and young_m1 are respectively the flux fraction and the mass fraction for $t < 0.102 \text{ Gyr}$, young_x2 and young_m2 are respectively the flux fraction and the mass fraction for $t < 24.5 \text{ Myr}$.

Num	(1)	(2)	(3)	(4)	(5)	(6)	(7)	(8)	(9)	(10)	(11)	(12)
Dis(pc)	-41.5	-37.4	-33.2	-29.1	-24.9	-22.8	-20.8	-18.7	-16.6	-14.5	-12.5	-8.3
Aper(pix)	2	2	2	2	1	1	1	1	1	1	1	2
Snr	6.7	7.8	7.4	8.4	14	15.3	11.4	13.8	10.1	14.3	17.7	8.8
χ^2	2.51	2.31	0.78	0.87	2.80	3.20	1.32	1.58	0.85	1.47	2.16	0.34
A_v	1.23	1.27	0.91	1.32	0.78	0.91	0.79	0.69	0.66	0.53	0.39	0.37
pl_x%	0.00	0.00	0.00	0.00	0.00	0.02	6.74	2.60	5.10	4.17	10.44	15.70
young_x1 (%)	0.22	0.00	15.95	15.74	65.24	80.52	80.81	58.67	46.20	42.90	16.55	8.97
young_x2 (%)	0.22	0.00	10.56	13.48	1.30	7.80	3.51	15.69	24.14	13.83	12.56	8.97
young_m1 (%)	0.001	0.00	0.257	1.042	2.716	4.501	5.407	2.247	1.496	1.540	0.294	0.048
young_m2 (%)	0.001	0.00	0.085	0.627	0.011	0.088	0.053	0.114	0.087	0.161	0.116	0.048
Num	(13)	(14)	(15)	(16)	(17)	(18)	(19)	(20)	(21)	(22)	(23)	(24)
Dis(pc)	-4.1	center	4.1	8.3	12.5	14.5	16.6	18.7	20.8	24.9	31.3	39.4
Aper(pix)	2	2	2	2	1	1	1	1	1	2	4	4
Snr	6.6	10.4	12.9	11.1	12.2	12.3	10	16.7	10.4	8.2	6.74	8
χ^2	0.20	0.71	1.52	0.57	1.24	0.92	0.59	1.87	0.83	0.36	0.35	1.64
A_v	0.41	0.82	1.45	1.21	1.01	0.74	0.70	0.37	0.53	0.76	1.27	1.46
pl_x%	21.58	15.09	19.88	14.94	0.00	7.45	1.42	0.00	3.74	3.84	0.0	0.00
young_x1 (%)	0.08	23.30	31.58	52.12	19.34	16.31	54.15	25.20	13.93	62.38	25.35	0.00
young_x2 (%)	0.00	0.00	4.14	11.72	19.30	16.07	14.13	11.88	13.93	0.01	7.71	0.00
young_m1 (%)	0.000	0.588	1.042	1.832	0.101	0.151	2.107	0.456	0.093	2.139	0.802	0.000
young_m2 (%)	0.000	0.000	0.038	0.112	0.100	0.140	0.04	0.08	0.09	0.000	0.080	0.000

4020 Å is about 5-15. Based on table 1 in Cid Fernandes et al. (2005), considering the "intermediate" and "old" ages, an uncertainty of 8-14% can be given for the flux-fraction and 7-10% for the mass-fraction. However, considering the "young" age, it is 1-2% and 4-7% for the flux-fraction, the mass-fraction, respectively. The uncertainty in the flux/mass fraction for the age of "young" is smaller than that for the ages of "intermediate" and "old". Therefore, 10% is adopted as their typical uncertainty. In our SSP fit, the power-law slope is fixed to -0.5. We tried other slopes, and found the result shows little change.

In Figure 4, the flux/mass fraction is shown as a function of distance from the nucleus of M51. It is found that the mean flux fraction of young stellar populations ($t < 24.5 \text{ Myr}$, the cyan line in Fig. 4) is about 9%, excluding some regions near the center (from -6 pc to 2 pc). Excluding these regions with a flux fraction from the young stellar population of zero (from -6 pc to 2 pc), the mean mass fraction is about 0.09%. If choosing $t < 0.102 \text{ Gyr}$, the mean flux fraction of young stellar populations is 34%, the mean mass fraction is 1.3%, and the mass fraction is also smaller in the central region (the red line in Fig. 4).

3.2 Specific star formation rate

Two widely employed methods to measure the current star formation rates (SFR) is by examining the ultraviolet continuum, and by using the emission lines of $H\alpha$, $[O II]$, etc. (Kennicutt, 1998). For a sample of 82302 star forming galaxies from SDSS, Asari et al. (2007) investigated the current SFR derived from the SSP synthesis and found that it is consistent with that from the $H\alpha$ SFR indicator. They found that the Spearman rank correlation coefficients applied to results show there is a strong correlation when the critical age is selected from 10 Myr to 0.1 Gyr. In our paper, the current specific SFR (SSFR) is defined by the mean SSFR over the past 24.5 Myr, i.e., the mass fraction of first 12 of

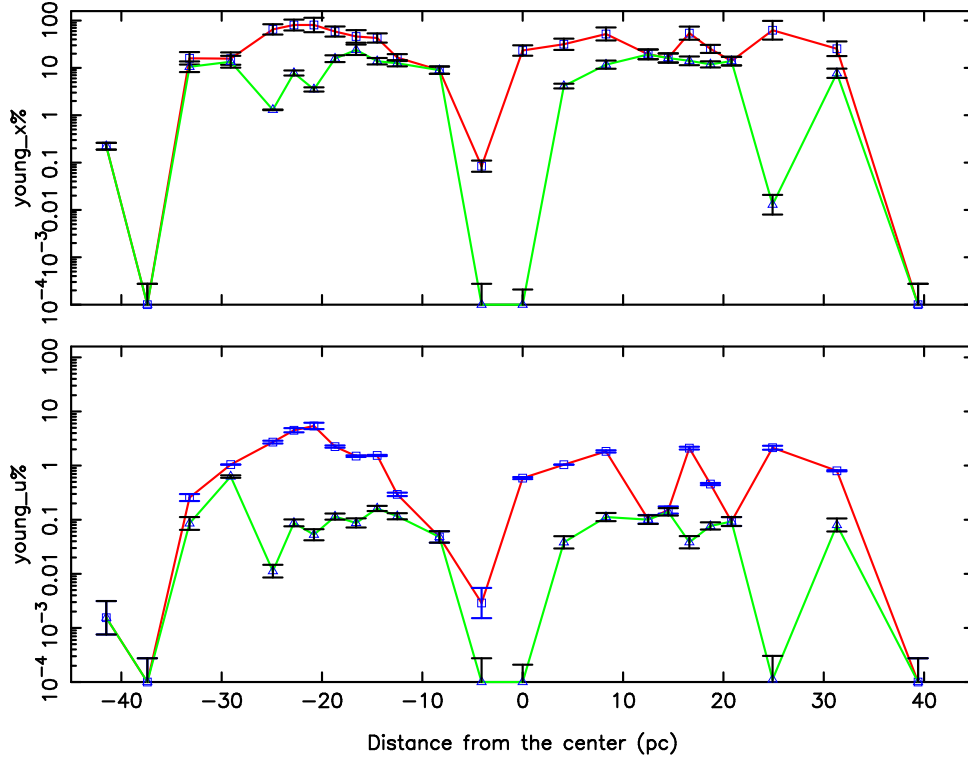


Fig. 4 Radial distributions of the flux fraction (top) and the mass fraction (bottom) of the young stellar population for $t < 0.102 \text{ Gyr}$ (the red line) and for $t < 24.5 \text{ Myr}$ (cyan line). The points on the x-axis give locations where no young stellar population is required in SSP model.

the 45 templates described in section 2.3 with age less than 24.5 Myr (Asari et al., 2007),

$$\text{SSFR}(t < 24.5\text{Myr}) = \frac{\text{SFR}}{M_*} = \frac{\sum_{j=1}^{12} \mu_j}{24.5\text{Myr}} \quad (2)$$

where M_* is the stellar mass.

The mean young mass fraction is 0.09% ($t < 24.5\text{Myr}$) and the current SSFR($t < 24.5\text{Myr}$) is about $0.037 \pm 0.004 \text{ Gyr}^{-1}$ (Table 2, Fig. 4). The young stellar populations are not required in the center inner $\sim 8 \text{ pc}$ in M51 (from -6.0 pc to 2.0 pc), suggesting a possible SSFR suppression in the circumnuclear regions from the feedback of the AGNs. Considering the young flux/mass fraction for $t < 0.102 \text{ Gyr}$ in stead of $t < 24.5 \text{ Myr}$, the mean young mass fraction is 1.3 % and the current SSFR($t < 0.102 \text{ Gyr}$) is about $0.13 \pm 0.013 \text{ Gyr}^{-1}$. The central SSFR is also smaller in the central region. We also found that there are dips in the SSFR at the edge of our measured region, around 40 pc away from the center.

The nucleus of M51 is selected between cloud 4 and cloud 5 following Bradley et al. (2004). Cloud 4 and cloud 5 are all at $\sim 7 \text{ pc}$ from the nucleus. In Fig. 14 of Bradley et al. (2004), they found that the radio jet (8.4GHz) is elongated with a position angle close to that of this measurement of M51 with the *HST* STIS slit. From Table 2 and Fig. 3, the region where young stellar populations are not required ($t < 24.5 \text{ Myr}$) is not symmetrical with respect to the nucleus along the STIS long slit. This suggests that the radial distribution of SSFR in M51 is not symmetrical with respect to the direction along the

long slit. The influence of AGN feedback on the circumnuclear region is not symmetrical. This unsymmetrical SSFR distribution is possibly due to the AGN jet in M51 (e.g. Bradley et al., 2004). Using the Submillimeter Array (SMA), which has a spatial resolution of ~ 10 pc, Matsushita (2013) found two highly disturbed CO(2-1) molecular gas features, which are perpendicular to the radio jet. These observations suggest the possible AGN feedback from the radio jet in M51. An AGN with strong jet activity can have less star formation in the circumnuclear regions, which is consistent with our result. In the future, integrated field unit (IFU) onboard the James Webb Space Telescope is needed to investigate the AGN-starburst connection in the circumnuclear region.

4 CONCLUSIONS

With the high spatial resolution provided by *HST* STIS (~ 2 pc), the radial stellar population in the inner ~ 40 pc for the nearby Seyfert 2 galaxy M51 is investigated. The main conclusions can be summarized as follows: (1) We present 24 radial optical spectra taken with the STIS long slit. These spectra cover the region extending $\sim 1''$ from the nucleus (i.e., -41.5 pc to 39.4 pc). (2) By SSP, the stellar contribution to these radial optical spectra is modeled. It is found that the mean flux fraction of young stellar populations (younger than 24.5 Myr) is about 9%. Excluding some positions near the center (from -6.0 to 2.0 pc), the mean mass fraction is about 0.09% and the mean SSFR is about 0.037 Gyr^{-1} . (3) These young stellar populations are not required to be in the center inner ~ 8 pc in M51, suggesting possible SFR suppression in the circumnuclear regions from the AGN feedback. (4) The radial distribution of SSFR in M51 is not symmetrical with respect to the STIS long slit, which implies that the influence of AGN feedback on the circumnuclear region is possibly not symmetrical. This unsymmetrical SSFR distribution is possibly due to the AGN jet in M51.

5 ACKNOWLEDGMENTS

We are grateful to the anonymous referee for instructive comments. This work has been supported by the National Science Foundations of China (Grant Nos. 11373024; 11233003; 11173016).

References

- Asari, N. V., et al., 2007, MNRAS, 381, 263
 Bradley, L. D., et al., 2004, ApJ, 603, 463
 Bian, W. H. & Huang K., 2010, MNRAS, 401, 507
 Bruzual, G., & Charlot S. 2003, MNRAS, 344, 1000
 Cardelli, J. A., Clayton G. C., & Mathis J. S. 1989, ApJ, 345, 245
 Chen, Y. M., et al., 2009, ApJ, 695, L130
 Cid Fernandes, R., Mateus, A., Sodre L., Stasinska, G., Gomes J., 2005, MNRAS, 358, 363
 Kennicutt, R. C., 1998, ARA&A, 36, 189
 Matsushita, S., 2013, Proceedings of "the Central Kiloparsec in Galactic Nuclei - Astronomy at High Angular Resolution 2011," to be appear in Journal of Physics: Conference Series (IOP Publishing), astro-ph/1205.0399
 Rice, M. S., et al., 2006, ApJ, 636, 654
 Spinelli, P. E., et al., 2006, ApJS, 166, 498
 Tremaine S., et al., 2002, ApJ, 574, 740
 Wang, J. M., et al., 2007, ApJ, 661, L143